State transition of a non-Ohmic damping system in a corrugated plane

Kun Lü and Jing-Dong Bao*

Department of Physics, Beijing Normal University, Beijing 100875, China

(Received 23 July 2007; published 20 December 2007)

Anomalous transport of a particle subjected to non-Ohmic damping of the power δ in a tilted periodic potential is investigated via Monte Carlo simulation of the generalized Langevin equation. It is found that the system exhibits two relative motion modes: the locked state and the running state. In an environment of sub-Ohmic damping ($0<\delta<1$), the particle should transfer into a running state from a locked state only when local minima of the potential vanish; hence a synchronization oscillation occurs in the particle's mean displacement and mean square displacement (MSD). In particular, the two motion modes are allowed to coexist in the case of super-Ohmic damping ($1<\delta<2$) for moderate driving forces, namely, where double centers exist in the velocity distribution. This causes the particle to have faster diffusion, i.e., its MSD reads $\langle\Delta x^2(t)\rangle=2D_{\text{eff}}^{(\delta)}t^{\delta_{\text{eff}}}$. Our result shows that the effective power index δ_{eff} can be enhanced and is a nonmonotonic function of the temperature and the driving force. The mixture of the two motion modes also leads to a breakdown of the hysteresis loop of the mobility.

DOI: 10.1103/PhysRevE.76.061119 PACS number(s): 05.70.Fh, 05.60.−k, 05.40.−a, 05.10.Ln

I. INTRODUCTION

There are many physical situations that can be described by Brownian transport in a tilted periodic potential, for example, Josephson junctions [1], charge-density waves [2], superionic conductors [3], rotation of dipoles in an external field [4], phase-locking loops [5], diffusion on surfaces [6], and separation of particles by electrophoresis [7]. The quantitative properties of those systems have been discussed in many papers [8], such as the dependence of the coherence level of transport on the temperature, driving force, and shape of the potential [9]; the huge enhancement of the effective diffusion coefficient relative to the free diffusion [10–12]; the response of output to the noise and signal [13]; and so on [14]. Since theoretical tools and numerical algorithms are not sufficient in non-Markovian dynamics with a frequency-dependent non-Ohmic damping, most models are established in an Ohmic damping environment. However, the frequency-dependent damping is more general because a large number of stochastic processes do not have Markovian dynamics.

Recent studies on anomalous diffusion and transport are mostly limited to the absence of potential, the linear force case, or subdiffusion in a potential [15]. It is worth pointing out that the behavior of a particle moving in a periodic potential immersed in a super-Ohmic damping environment might be far more complicated than that in the Ohmic and sub-Ohmic damping cases. In comparison with the previous findings of great enhancement of the effective diffusion coefficient [10–12] and the hysteresis loop of mobility [8] in the Ohmic damping environment, we will perform a detailed investigation in the present work of the diffusion and the mobility of a particle subjected to arbitrary non-Ohmic damping in a corrugated plane. This is in terms of an effective algorithm proposed by us [16] to numerically solve a generalized Langevin equation (GLE) with an arbitrary damping kernel function and corresponding thermal colored noise.

The paper is organized as follows. In Sec. II, we describe briefly the anomalous transport model by means of the GLE. In Sec. III, the two basic quantities of interest, the generalized effective diffusion coefficient and the fractional mobility, are defined; the behaviors of diffusion and mobility are shown. Finally, we draw a conclusion in Sec. IV.

II. THE MODEL

We consider a Brownian particle moving in a one-dimensional periodic potential under the influence of non-Ohmic memory friction and a constant external driving force. The dynamics of the particle is governed by the following GLE [17,18]:

$$\dot{x}(t)=v(t),$$

$$m\dot{v}(t)=-m\int_0^t\gamma(t-t')v(t')dt'+U'(x)+\sqrt{mk_BT}\xi(t), \tag{1}$$

where k_B is the Boltzmann constant, T is the temperature of the environment, and $\gamma(t)$ is the damping kernel function, related to $\xi(t)$ through the fluctuation-dissipation theorem [17,19]

$$\langle\xi(t)\xi(t')\rangle=\gamma(|t-t'|), \tag{2}$$

where $\xi(t)$ is a zero mean Gaussian colored noise with spectral density

$$\langle|\xi(\omega)|^2\rangle=2\gamma_\delta\left(\frac{|\omega|}{\tilde{\omega}}\right)^{\delta-1}f_c\left(\frac{|\omega|}{\omega_c}\right). \tag{3}$$

The small-$|\omega|$ behavior of $\langle|\xi(\omega)^2|\rangle$ is a power law characterized by the index $\delta-1$. The function $f_c(|\omega|/\omega_c)$ is a high-frequency cutoff function of typical width ω_c [20], and

*Corresponding author. jdbao@bnu.edu.cn

$\tilde{\omega} \ll \omega_c$ denotes a reference frequency allowing for the constant $m\gamma_\delta$ to have the dimension of viscosity for any δ [21]. The cases of $0<\delta<1$ and $1<\delta<2$ are sub-Ohmic and super-Ohmic damping, respectively; $\delta=1$ is the Ohmic case. In Eq. (1), $U(x)$ is considered to be a tilted periodic potential,

$$U(x) = -U_0 \cos\left(\frac{2\pi}{\lambda}x\right) - Fx. \tag{4}$$

The minima of $U(x)$ vanish when the driving force F is taken to be the critical value: $F_c = U_0 2\pi/\lambda = 1.0$.

In the calculation, natural units ($m=1$ and $k_B=1$), the dimensionless parameters $U_0=1.0$, $\lambda=2\pi$, $\gamma_\delta=4.0$, the smooth cutoff function $f_c=\exp(-\omega/\omega_c)$ [21] with $\omega_c=4.0$, and the time step $\Delta t=0.01$ are used. The test particles start from the origin of coordinates and have zero velocity; here 2×10^4 test particles are used to describe the stochastic distribution of a Brownian particle.

III. DIFFUSION AND MOBILITY

The quantities of foremost interest are the diffusion coefficient and the mobility. Here we generalize both to the non-Ohmic damping case with an arbitrary power index δ,

$$D^{(\delta)} := \lim_{t\to\infty}\frac{1}{\Gamma(1+\delta)}\, {}_0D_t^{\delta}\langle \Delta x^2(t)\rangle_\delta, \tag{5}$$

$$\mu_\delta := \lim_{t\to\infty}\frac{1}{F\sin(\delta\pi/2)}\, {}_0D_t^{\delta}\langle x(t)\rangle_\delta, \tag{6}$$

where ${}_0D_t^{\delta}$ denotes the fractional derivative. The algorithm for numerically calculating the two quantities is presented in the Appendix.

A. Diffusion

We begin our studies from the situation of sub-Ohmic damping. The case of sub-diffusion dynamics has been discussed by Goychuk and Hänggi [22], where the GLE and the fractional Fokker-Planck equation approaches to the escape dynamics are used and compared. The escape is governed asymptotically by a power law whose exponent depends exponentially on both the barrier height and the temperature. If the ratio of the barrier height to the temperature is too large, the diffusion motion in a washboard potential well below a critical tilt cannot be observed numerically within a reasonable time window, i.e., nearly all the test particles are confined in the locked state. Therefore, we consider the transport of a sub-Ohmic damped particle subjected to a large driving force because of the efficiency of the numerical simulation of the GLE. Figures 1(a) and 1(b) show the time-dependent mean square displacement (MSD) and mean displacement of the particle of $\delta=0.6$. When the driving force F is increased until local minima of the potential vanish, we find that the MSD of the particle shows a quasiperiodic oscillation. As long as the MSD of the particle experiences a quasiperiodic process, the particle will move the distance of a periodic length $\Delta x=2\pi$ along the direction of the external force.

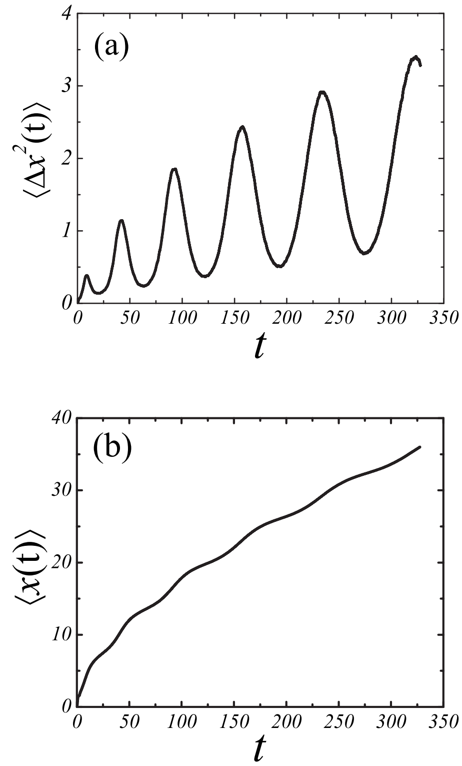

FIG. 1. (a) Time-dependent MSD of a sub-Ohmic damped particle of $\delta=0.6$ and (b) its mean displacement. The parameters used are $F=5.0$ and $T=0.1$.

In Fig. 2, we plot the space probability distribution of a sub-Ohmic damped particle at different times. It is seen that, with the evolution of time, the width of the probability distribution becomes narrow periodically when the particle moves in the bottom of a potential well; it is broad when the particle arrives at the top of the potential. Unlike the normal Ohmic damped particle [10], its probability distribution is centralized. Our results can be interpreted as follows. In the sub-Ohmic damping environment, the particle has a strong memory of its initial position and thus the diffusion in the coordinate space is very slow. If the potential have local minima, it is quite difficult for the particle to escape from the potential well, thus the particle is in a locked state during the period of simulation. As the local minima of the potential

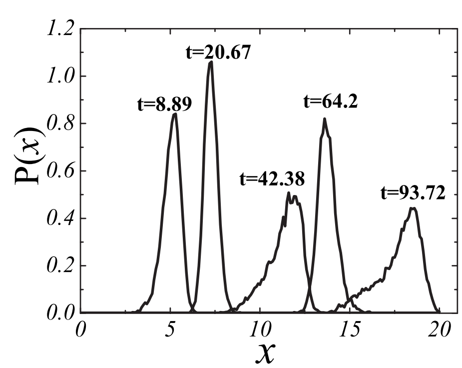

FIG. 2. Space probability distribution of a sub-Ohmic damped particle of $\delta=0.6$ at different times for $F=5.0$ and $T=0.1$.

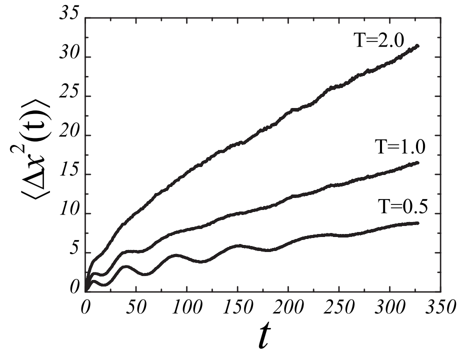

FIG. 3. MSD of the particle with $\delta=1.7$ at a large driving force $F=5.0$ for various temperatures.

vanish, the particle subjected to a large driving force can enter the running state. Therefore, its distribution width is modulated by the periodic structure of the potential and thus the MSD of the particle has a quasiperiodic oscillation.

Figure 3 shows that the quasiperiodic oscillation phenomenon becomes inconspicuous when the temperature increases for $T>1.0$ at $F=5.0$. In this case the particle transfers completely into the running state and hence the structure of the potential might have less influence on the transport process.

In particular, in the case of super-Ohmic damping, we find numerically that the asymptotic MSD of the particle can be approximately written as a power function,

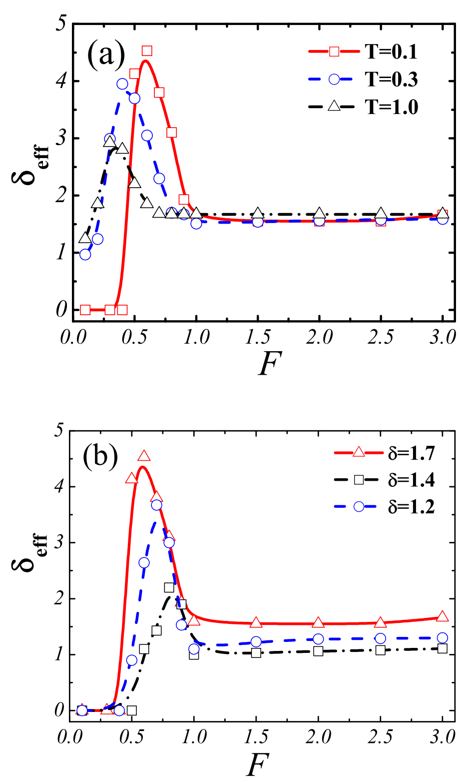

FIG. 4. (Color online) (a) Effective power index δ_{eff} vs F for various T at $\delta=1.7$. (b) Effective power index vs F for various δ at $T=0.1$.

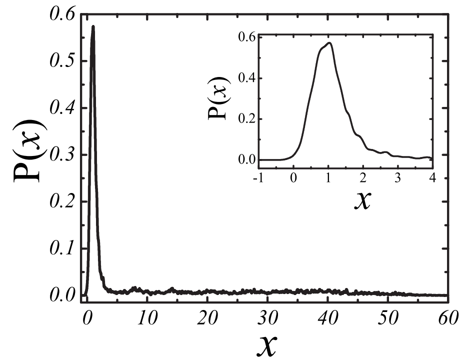

FIG. 5. Space probability distribution of the particle at time $t=50.0$. The inset figure is the probability distribution in the locked state only. The parameters used are $\delta=1.7$, $F=0.75$, and $T=0.1$.

$$\langle \Delta x^2(t)\rangle = 2D_{\mathrm{eff}}^{(\delta)} t^{\delta_{\mathrm{eff}}(T,F)}, \tag{7}$$

where δ_{eff} depends on T and F. Indeed, the index δ_{eff} is not always equal to δ as for the Ohmic and the sub-Ohmic damping cases, but varies nonmonotonically with F. For a moderate F, we find an interesting result. The effective power index δ_{eff} exceeds 2 (i.e., ballistic diffusion [23–25]) when the periodic potential is tilted observably but its local minima still exist. Further analysis shows that the mysterious diffusion behavior is caused by the mixing of the locked and the running states.

In Figs. 4(a) and 4(b), we plot the effective power index δ_{eff} as a function of F for various T and δ. It is seen from Fig. 4(a) that the maximal value of δ_{eff} versus F forward with increasing temperature. Similar behavior of δ_{eff} for other super-Ohmic damping cases can also be observed, as shown in Fig. 4(b). The smaller the value of δ, the larger is F where the maximum δ_{eff} appears. This can be interpreted qualitatively as follows. In the non-Markovian rate theory [26], for a sufficiently big ratio of barrier height to temperature, superdiffusion in a periodic potential should turn into normal diffusion because the escape events are exponentially distributed in time and no overlong jumps can occur, so that $\delta_{\mathrm{eff}}=1$ when the tilt of the potential is small. Also, for very large F and vanishing structure effect of the potential, all the test particles can move into a running state, thus $\delta_{\mathrm{eff}}=\delta$. However, for a medium tilt, some test particles are confined in the potential well (in the locked state) and others drift quickly forward (in the running state). A proper proportion between the locked state and the running state should induce the maximum of the effective power index. Clearly, it becomes easier for the particle in the locked state to escape the well and join the running state with increase of either T or δ. Therefore, the maximum of δ_{eff} appears in the case of a small F at high temperature, and in the case of large δ at low temperature.

In Fig. 5, we illustrate the case of $\delta=1.7$ at low temperature ($T=0.1$) and middle tilt ($F=0.75$) to depict the coexistence of the two motion modes. The backward and forward barrier heights are given by

$$U_1 = 2U_0\sqrt{1-\left(\frac{F\lambda}{2\pi U_0}\right)^2} + \frac{F\lambda}{\pi}\arcsin\left(\frac{F\lambda}{2\pi U_0}\right) + \frac{F\lambda}{2},$$

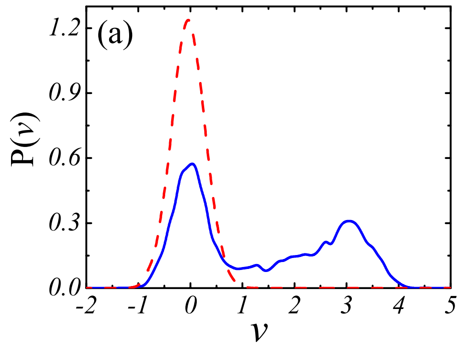

FIG. 6. (Color online) Velocity distributions of the particle at $t=150$ (a) and 330 (b). The solid and dashed lines are the results of the super-Ohmic $\delta=1.7$ and Ohmic $\delta=1.0$ cases, respectively. The parameters used are $F=0.75$ and $T=0.1$.

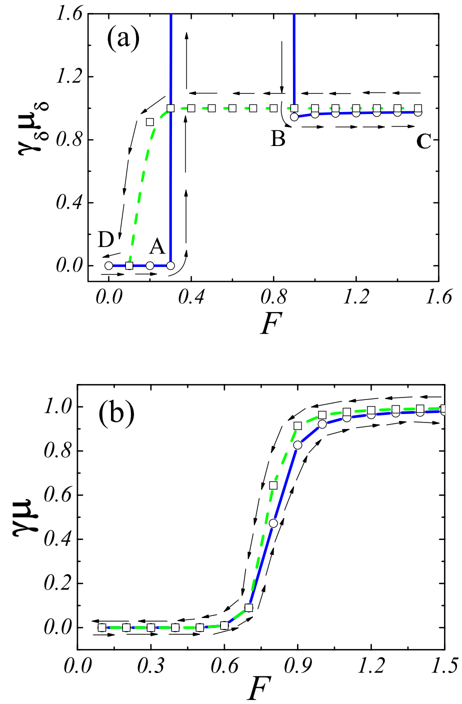

FIG. 7. (Color online) (a) Fractional mobility times damping constant as a function of driving force in the super-Ohmic damping case with $\delta=1.7$. (b) Normal Ohmic damping result with $\gamma=0.5$. The solid and dashed lines correspond to the forward and backward processes, respectively. The temperature is $T=0.1$.

$$U_2 = 2U_0\sqrt{1-\left(\frac{F\lambda}{2\pi U_0}\right)^2} + \frac{F\lambda}{\pi}\arcsin\left(\frac{F\lambda}{2\pi U_0}\right) - \frac{F\lambda}{2}. \tag{8}$$

For a low temperature $T < U_2 \ll U_1$, the particle oscillates around the potential well; however, it still escapes over a barrier with a small probability. Since the barrier crossing process is quite slow at low temperature, the particle in the locked state has an approximate Gaussian space distribution centered at x_0 [$x_0=(\lambda/2\pi)\arcsin(F\lambda/2\pi U_0)$], as shown in the inset of Fig. 5. Once the test particle climbs over the barrier, it will no longer be restricted again. Because the next hill of the tilted periodic potential is lower than the present one, the kinetic energy of the particle gained from the external driving force is greater than the dissipated energy due to the memory friction. The particle can enter the running state, so it drifts quickly along the direction of the driving force. This results in a long tail appearing in the space probability distribution of the particle. For the Ohmic damped particle, once escaped over a barrier, it will slide to the next well and be trapped again. Hence the space probability distribution of the Ohmic damped particle disintegrates into small pieces and does not make up a running state.

Figures 6(a) and 6(b) show the coexistence of the two motion modes of the super-Ohmic damped particle, which can be seen for the velocity distributions of the particle at times $t=150$ and 330. As expected, we do not find the coexistence phenomenon of two velocity modes appearing in the normal diffusion. It is seen that the super-Ohmic damped particle enters the running state with an increasing probability; the difference between the two center velocities in the running and rocking states becomes large with the evolution of time. This implies that, as long as the test particles escape out of the well, they will be accelerated by the corrugated plane and join the running state. Of course, the present locked state occurs simply because we cannot observe the motion on the time scale of our numerical simulation as the escape rate is very low [22], but a new locked state relative to the forward running state should arise once the original locked state disappears.

B. Mobility

The mobility determined by Eq. (6) as a function of the driving force is plotted in Fig. 7. Starting from zero tilt and switching on the tilt F adiabatically, the mobility of the particle remains zero when all the test particles are in the locked state until some of them join the running state. In comparison with the Ohmic damping case, we find that the hysteresis loop is broken and becomes staggered. At that point A, the mobility jumps to infinity and then drops to a constant at point B and remains constant with increasing F (point C). The point B corresponds to the critical force $F=F_c$, where the local minima of the corrugated plane vanish. When the driving force decreases adiabatically, all the test particles are kept in the running state and the mobility approaches a constant, until the driving force becomes so small that most of the test particles are trapped in the potential wells. At the point D, the mobility falls to zero again. However, for the usual Ohmic damping case shown in Fig. 7(b), we find that bistability occurs in the region $0.7 < F < 1.4$, which forms a hysteresis loop. However, for the sub-Ohmic damping case, we have not found a similar hysteresis loop of mobility like the one that arises in the Ohmic damping case.

IV. SUMMARY

We have investigated the transport of a non-Ohmic damped particle in a tilted periodic potential and reported an interesting finding: The tilted periodic potential as a simple equipment which not only enhances the diffusion coefficient, but also changes the diffusive behavior of the particle. This is due to the phenomenon of two motion modes: the locked and the running states, which can appear and transform from one to the other in the corrugated plane. In the sub-Ohmic damping case, the mean square displacement of the particle shows a quasiperiodic property when the driving force is larger than the critical value where the minima of the potential vanish. For the super-Ohmic damping case, the two motion modes can coexist and transform from one to the other (that is, there exist two centers in the velocity distribution). Thus the power index for the mean square displacement of the particle is enhanced. In comparison with the hysteresis loop of mobility of the normal case, the hysteresis loop of mobility of a super-Ohmic damping particle is broken.

The anomalous Brownian motion in a periodic potential is useful for many applications occurring in areas such as condensed matter physics, chemical physics, molecular biology, communication theory, and so on. We are confident that both theoretical and experimental works in the future will help in further clarification of all these intriguing issues and problems.

ACKNOWLEDGMENTS

This work was supported by the National Natural Science Foundation of China under Grant No. 1067401 and the Specialized Research Foundation for the Doctoral Program of Higher Education under Grant No. 20050027001.

APPENDIX: NUMERICAL METHODS FOR FRACTIONAL CALCULUS

The so-called Riemann-Liouville fractional integral is defined through [27]

$$ {}_{t_0}I_t^{-\delta} f(t) = \frac{1}{\Gamma(\delta)} \int_{t_0}^{t} dt' \frac{f(t')}{(t-t')^{1-\delta}}, \quad t > 0, \quad \delta > 0, \tag{A1}$$

whereas its left inverse ${}_{t_0}D_t^{\delta}$ reads

$$ {}_{t_0}D_t^{\delta} := {}_0D_t^m \, {}_{t_0}I_t^{\delta-m}, \quad m-1 < \delta < m, \quad m \in \mathbb{N}, \tag{A2}$$

where ${}_0D_t^m$ denotes the ordinary derivative of order m. In this present work, the case of $t_0=0$ is concerned. For completeness, we define

$$ {}_0I_t^0 = {}_0D_t^0 = \mathbf{I}, \tag{A3}$$

where $\mathbf{I}$ is the identity operator. It is convenient to make use of the discrete operators of translation (shift) and finite differences to derive the approximate recursive expressions for the fractional differentiation operator ${}_0D_t^{\delta}$. The theory of numerical differentiation and integration (with equidistant grid points) has been developed clearly in Chaps. 7–10 of Ref. [28]. See also Chap. 6 of Ref. [29].

Let $\tau \in \mathbb{R}$. We define the shifting operator E^{τ} and the backward difference operator ∇_{τ} by their actions on a function $u(t)$ for $t \in \mathbb{R}$,

$$ E^{\tau}u(t) = u(t+\tau), \quad \nabla_{\tau}u(t) = u(t) - u(t-\tau). \tag{A4}$$

We furthermore have the relation, with $\mathbf{I}$ as the identity operator,

$$ \nabla_{\tau} = \mathbf{I} - E^{-\tau}. \tag{A5}$$

Using these notations, we write the approximation $[u(t) - u(t-\tau)]/h$ for the derivative $u'(t)$ of a differentiable function $u(t)$ as $\nabla_h u(t)/h$ for a small positive h, with accuracy $O(h)$ as the function $u(t)$ is sufficiently smooth. High-order derivatives $u^{(n)}(t) = {}_0D_t^n u(t)$ $(n \in \mathbb{N})$ with small $h > 0$ can be approximated by

$$ [\nabla_h^{(n)} u(t)]/h^n = h^{-n}(\mathbf{I} - E^{-h})^n u(t), \tag{A6}$$

again in the case of sufficiently smooth $u(t)$, with order of accuracy $O(h)$. The powers $\nabla_h^{(n)}$ can be readily expanded via the binomial theorem,

$$ \nabla_h^{(n)} = \sum_{j=0}^{n} (-1)^j \binom{n}{j} E^{-jh}. \tag{A7}$$

This leads to the known formula

$$ h^{-n} \sum_{j=0}^{n} (-1)^j \binom{n}{j} u(t-jh) = {}_0D_t^n u(t) + O(h). \tag{A8}$$

The remarkable fact now is that these formulas can be generalized to the case of noninteger order of the derivative. Replacing the positive integer n by a positive real number δ amounts to using the formal power

$$ \nabla_h^{\delta} = \sum_{j=0}^{\infty} (-1)^j \binom{\delta}{j} E^{-jh}, \tag{A9}$$

in analogy to the expansion (E^{-h} replaced by the complex variable z)

$$ (1-z)^{\delta} = \sum_{j=0}^{\infty} (-1)^j \binom{\delta}{j} z^j, \tag{A10}$$

which is convergent if $|z|<1$. We thus get the Grünwald-Letnikov approximation:

$$h^{-\delta}\nabla_h^\delta u(t) = h^{-\delta}\sum_{j=0}^{\infty}(-1)^j\binom{\delta}{j}u(t-jh) = {}_0D_t^\delta u(t) + O(h). \tag{A11}$$

If $u(t)$ decays to zero sufficiently fast as $t\to\infty$, in particular if $u(t)=0$ for $t<0$, ∇_h^δ will not diverge, and hence for the latter case we have

$$h^{-\delta}\nabla_h^\delta u(t) = h^{-\delta}\sum_{j=0}^{[t/h]}(-1)^j\binom{\delta}{j}u(t-jh). \tag{A12}$$

By using the property of the Gamma function

$$\Gamma(\delta)\Gamma(1-\delta) = \frac{\pi}{\sin(\pi\delta)},$$

we obtain the final recursion of the fractional calculus:

$${}_0D_t^\delta u(kh) = \frac{h^{-\delta}}{\Gamma(-\delta)}\sum_{j=0}^{k-1}\frac{\Gamma(j-\delta)}{\Gamma(j+1)}u[(k-j)h]. \tag{A13}$$

[1] A. Barone and G. Paterno, *Physics and Applications of the Josephson Effect* (Wiley, New York, 1982).

[2] G. Gruner, A. Zawadowski, and P. M. Chaikin, Phys. Rev. Lett. **46**, 511 (1981).

[3] P. Fulde, L. Pietronero, W. R. Schneider, and S. Strässler, Phys. Rev. Lett. **35**, 1776 (1975).

[4] D. Reguera, J. M. Rubi, and A. Pérez-Madrid, Phys. Rev. E **62**, 5313 (2000).

[5] W. C. Lindsey, *Synchronization Systems in Communication and Control* (Prentice-Hall, Englewood Cliffs, NJ, 1972).

[6] D. Agassi and J. H. Eberly, Phys. Rev. Lett. **54**, 34 (1985).

[7] A. Ajdari and J. Prost, Proc. Natl. Acad. Sci. U.S.A. **88**, 4468 (1992); G. I. Nixon and G. W. Slater, Phys. Rev. E **53**, 4969 (1996).

[8] H. Risken, *The Fokker-Planck Equation* (Springer, Berlin, 1984).

[9] E. Heinsalu, R. Tammelo, and T. Örd, Physica A **340**, 292 (2004).

[10] P. Reimann, C. Van den Broeck, H. Linke, P. Hänggi, J. M. Rubi, and A. Pérez-Madrid, Phys. Rev. Lett. **87**, 010602 (2001).

[11] D. Dan and A. M. Jayannavar, Phys. Rev. E **66**, 041106 (2002).

[12] P. Reimann, C. Van den Broeck, H. Linke, P. Hänggi, J. M. Rubi, and A. Pérez-Madrid, Phys. Rev. E **65**, 031104 (2002).

[13] D. Reguera, P. Reimann, P. Hänggi, and J. M. Rubi, Europhys. Lett. **57**, 644 (2002).

[14] B. Linder, M. Kostur, and L. Schimansky-Geier, Fluct. Noise Lett. **1**, R25 (2001); A. Buonocore and L. M. Ricciardi, Math. Biosci. **182**, 135 (2003); J. Kallunki, M. Dubé, and T. Ala-Nissila, Surf. Sci. **460**, 39 (2000); Q. Thommen, J. C. Garreau, and V. Zehnlé, Phys. Rev. A **65**, 053406 (2002).

[15] E. Heinsalu, M. Patriarca, I. Goychuk, G. Schmid, and P. Hänggi, Phys. Rev. E **73**, 046133 (2006); I. Goychuk, E. Heinsalu, M. Patriarca, G. Schmid, and P. Hänggi, *ibid.* **73**, 020101 (2006); E. Heinsalu, M. Patriarca, I. Goychuk, and P. Hänggi, J. Phys.: Condens. Matter **19**, 065114 (2007).

[16] K. Lü and J. D. Bao, Phys. Rev. E **72**, 067701 (2005); J. D. Bao, Y. Abe, and Y. Z. Zhuo, J. Stat. Phys. **90**, 1037 (1998).

[17] *Tokyo Summer Lectures in Theoretical Physics*, edited by R. Kubo (Benjamin, New York, 1966); R. Kubo, Rep. Prog. Phys. **29**, 255 (1966).

[18] R. Kubo, M. Toda, and N. Hashitsume, *Statistical Physics II: Nonequilibrium Statistical Mechanics*, 2nd ed. (Springer, Berlin, 1991).

[19] R. Muralidhar, D. J. Jacobs, D. Ramkrishna, and H. Nakanishi, Phys. Rev. A **43**, 6503 (1991).

[20] H. Grabert, P. Schramm, and G.-L. Ingold, Phys. Rev. Lett. **58**, 1285 (1987); Phys. Rep. **168**, 115 (1988).

[21] U. Weiss, *Quantum Dissipative Systems*, 2nd ed. (World Scientific, Singapore, 1999).

[22] I. Goychuk and P. Hänggi, Phys. Rev. Lett. **99**, 200601 (2007).

[23] J. D. Bao and Y. Z. Zhuo, Phys. Rev. Lett. **91**, 138104 (2003).

[24] J. D. Bao and Y. Z. Zhuo, Phys. Rev. E **71**, 010102(R) (2005).

[25] J. D. Bao, P. Hänggi, and Y. Z. Zhuo, Phys. Rev. E **72**, 061107 (2005).

[26] P. Hänggi, P. Talkner, and M. Borkovec, Rev. Mod. Phys. **62**, 251 (1990).

[27] S. G. Samko, A. A. Kilbas, and O. L. Marichev, *Fractional Integrals and Derivatives—Theory and Applications* (Gordon and Breach, New York, 1993); K. B. Oldham and J. Spanier, *The Fractional Calculus* (Academic, New York, 1974); K. S. Miller and B. Ross, *An Introduction to the Fractional Calculus and Fractional Differential Equations* (Wiley, New York, 1993); R. Hilfer, *Applications of Fractional Calculus in Physics* (World Scientific, Singapore, 1999).

[28] C. E. Fröberg, *Introduction to Numerical Analysis*, 2nd ed. (Addison-Wesley, Reading, MA, 1973).

[29] E. Isaacson and H. B. Keller, *Analysis of Numerical Methods* (Wiley, New York, 1966).